International Journal of Automotive Technology, Vol. 8, No. 6, pp. 753–760 (2007)

1229-9138/2007/037-10

ROLL AND PITCH ESTIMATION VIA AN ACCELEROMETER ARRAY AND SENSOR NETWORKS

W. BAEK[1], B. SONG[1]*, Y. KIM[2] and S.-K. HONG[2]

[1]Department of Mechanical Engineering, Ajou University, Gyeonggi 443-749, Korea
[2]Department of Electronic Engineering, Ajou University, Gyeonggi 443-749, Korea

(Received 12 March 2007; Revised 14 August 2007)

ABSTRACT–In this paper, a roll and pitch estimation algorithm using a set of accelerometers and wireless sensor networks (S/N) is presented for use in a passenger vehicle. While an inertial measurement unit (IMU) is generally used for roll/pitch estimation, performance may be degraded in the presence of longitudinal acceleration and yaw motion. To compensate for this performance degradation, a new roll and pitch estimation algorithm is proposed that uses an accelerometer array, global positioning system (GPS) and in-vehicle networks to get information from yaw rate and roll rate sensors. Angular acceleration and roll and pitch approximation are first calculated based on vehicle kinematics. A discrete Kalman filter is then applied to estimate both roll and pitch more precisely by reducing noise from the running engine and from road disturbance. Finally, the feasibility of the proposed algorithm is shown by comparing its performance experimentally with that of an IMU in the framework of an indoor test platform as well as a test vehicle.

KEY WORDS : Accelerometer array, Roll estimation, Pitch estimation, Kalman filter, Sensor networks

NOMENCLATURE

θ : pitch, [rad]
ϕ : roll, [rad]
ψ : yaw, [rad]
$\dot{\theta}$: pitch rate, [rad/s]
$\dot{\phi}$: roll rate, [rad/s]
$\dot{\psi}$: yaw rate, [rad/s]
$\ddot{\theta}$: angular acceleration of pitch, [rad/s^2]
$\ddot{\phi}$: angular acceleration of roll, [rad/s^2]
$\ddot{\psi}$: angular acceleration of yaw, [rad/s^2]
P_m : measurement of $\ddot{\theta}$, [rad/s^2]
Q_m : measurement of $\dot{\phi}$, [rad/s]
P_{bias}, Q_{bias} : measurement bias
w_θ, w_ϕ : process noise
v_θ, v_ϕ : measurement noise
g : gravity, [m/s^2]
Δt : sampling time, [sec.]

SUBSCRIPTS
A, B, C : sensor nodal point
G : center of rotation
l, *r* : left, right
fr, *rr* : front, rear

*Corresponding author. e-mail: bsong@ajou.ac.kr

1. INTRODUCTION

As an interest in active safety systems for a passenger vehicles has increased, multiple sensor types have been developed and implemented to obtain information on vehicle dynamics. In particular, inertial sensors such as accelerometers and gyroscopes have received much attention, with applications ranging from front/side crash sensing for airbag control and roll stability control to automotive navigation systems (Kim *et al.*, 2006; Ungoren and Peng, 2004; Siemens, 2007; VTI, 2007). However, the devices and sensors for active safety systems have until recently been designed separately and independently, as shown in Figure 1 (Siemens, 2007; VTI, 2007; Bosch, 2007). The primary reason for this may come from the fact that large automobile manufactures subcontract the supply of the active safety devices and systems to smaller scale manufactures (Mostov *et al.*, 1997). While many of the active safety systems are in general operated independently, most of them rely on the same types of micro electro mechanical system (MEMS) inertial sensors (refer to Figure 1) and a full integration of these sensors will be the logical and inevitable direction to reduce cost in the near future.

Over the last decade, much effort has been made to estimate both roll and pitch angle, as these values represent key information for active safety control of a vehicle. Most of the approaches in the literature are based

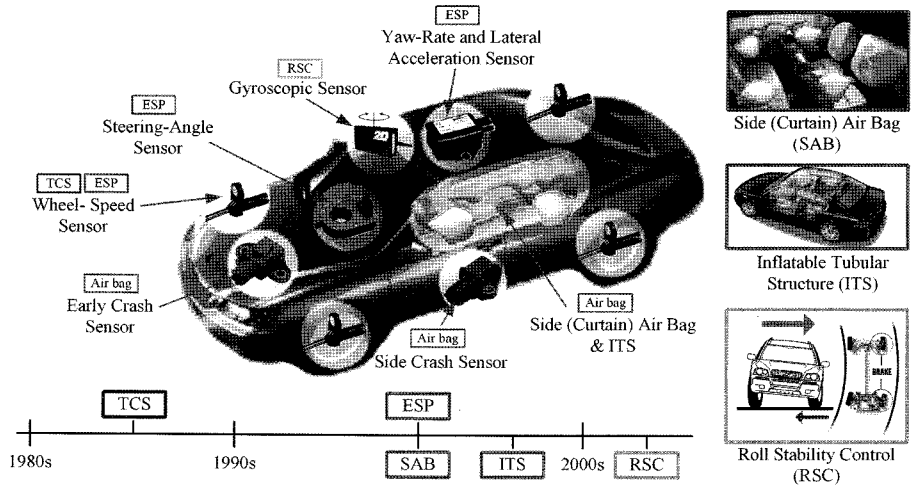

Figure 1. Sensor layout for active safety systems.

on either GPS or IMU. For instance, Ryu and Gerdes proposed a method to measure road bank angle and road grade by using GPS with multiple antennas (Ryu and Gerdes, 2004). However, this approach requires intensive computation to process the data of multiple antenna GPS compared to that of single antenna GPS. Another roll/pitch estimation algorithm using an IMU and wheel speed sensing was proposed by Tseng *et al.* (2007). In emergency situations with large acceleration or deceleration, however, the performance can be degraded.

The contributions of this paper are twofold: the first is to develop the estimation algorithm of roll and pitch for a passenger vehicle using an accelerometer array and single antenna GPS, and the second is to validate the estimation algorithm experimentally. More specifically, the signal processing algorithm will be combined with a discrete Kalman filter to cancel out both sensor measurement noise and disturbances resulting from the running engine and the terrain. The feasibility of the roll and pitch estimation algorithm will then be validated by comparing its performance experimentally with that of a certain IMU in the framework of an indoor test platform and a real vehicle.

2. PROBLEM STATEMENT

In this section, vehicle kinematics are described under a rigid-body assumption. Equations to calculate both roll and pitch are then derived based on the kinematics, and two technical problems related to the equations are discussed. Finally, a sensor layout for estimating both roll and pitch is described.

2.1. Kinematics of Vehicle

To derive the kinematics of the passenger vehicle, two coordinate systems are considered: one is a fixed inertial coordinate system $\mathbf{I} = \{O : \vec{e}_1, \vec{e}_2, \vec{e}_3\}$ where O is the origin and $\{\vec{e}_1, \vec{e}_2, \vec{e}_3\}$ is a right-handed orthonormal basis. The other is a body-fixed coordinate system $\mathbf{B} = \{G : \vec{b}_1, \vec{b}_2, \vec{b}_3\}$ where $\{\vec{b}_1, \vec{b}_2, \vec{b}_3\}$ is a right-handed orthonormal basis fixed on the rigid body. Then, as shown in Figure 2, the displacement vector at a point A with respect to the origin O is written as

$$\vec{r}_A = \vec{r}_{G/O} + \vec{r}_{A/G} = \vec{r}_{G/O} + x_{fr}\vec{b}_1 + y_l\vec{b}_2 + z_{fr}\vec{b}_3 \tag{1}$$

where $\vec{r}_{G/O}$ is the displacement vector from O to G with respect to the fixed inertial coordinate **I** and $\vec{r}_{A/G}$ is the vector from G to A with respect to the body-fixed system **B**.

With the angular velocity and acceleration at point G are given respectively as

$$\omega_b = \dot{\phi}\vec{b}_1 + \dot{\theta}\vec{b}_2 + \dot{\psi}\vec{b}_3\,, \quad \alpha_b = \ddot{\phi}\vec{b}_1 + \ddot{\theta}\vec{b}_2 + \ddot{\psi}\vec{b}_3 \tag{2}$$

the acceleration at the point A can be written as

$$\begin{aligned}\vec{a}_A = {} & \ddot{\vec{r}}_{G/O} \\ & + \left[-x_{fr}\left(\dot{\theta}^2 + \dot{\psi}^2\right) + y_l\left(\dot{\theta}\dot{\phi} - \ddot{\psi}\right) + z_{fr}\left(\dot{\phi}\dot{\psi} - \ddot{\theta}\right)\right]\vec{b}_1 \\ & + \left[x_{fr}\left(\dot{\theta}\dot{\phi} + \ddot{\psi}\right) - y_l\left(\dot{\phi}^2 - \dot{\psi}^2\right) + z_{fr}\left(\dot{\phi}\dot{\psi} - \ddot{\theta}\right)\right]\vec{b}_2 \\ & + \left[x_{fr}\left(\dot{\phi}\dot{\psi} - \ddot{\theta}\right) + y_l\left(\dot{\theta}\dot{\psi} + \ddot{\phi}\right) - z_{fr}\left(\dot{\phi}^2 + \dot{\theta}^2\right)\right]\vec{b}_3\end{aligned} \tag{3}$$

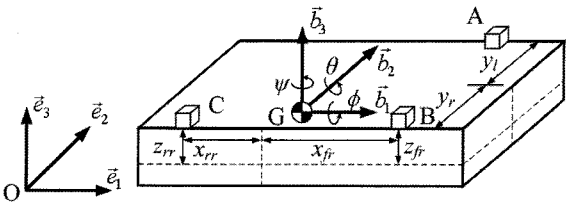

Figure 2. Coordinates and notations used to describe vehicle kinematics.

Assuming that the points A and B are in the same line along the $\vec{b}_2$ axis and the points B and C are also in the same line along the $\vec{b}_1$ axis, the accelerations at the points B and C, respectively, are similarly derived as follows:

$$\begin{aligned}\vec{a}_B = & \ddot{\vec{r}}_{G/O} \\ & + \left[-x_{fr}\left(\dot{\theta}^2+\dot{\psi}^2\right)-y_r\left(\dot{\theta}\dot{\phi}-\ddot{\psi}\right)+z_{fr}\left(\dot{\phi}\dot{\psi}-\ddot{\theta}\right)\right]\vec{b}_1 \\ & + \left[x_{fr}\left(\dot{\theta}\dot{\phi}+\ddot{\psi}\right)+y_r\left(\dot{\phi}^2-\dot{\psi}^2\right)+z_{fr}\left(\dot{\phi}\dot{\psi}-\ddot{\theta}\right)\right]\vec{b}_2 \\ & + \left[x_{fr}\left(\dot{\phi}\dot{\psi}-\ddot{\theta}\right)-y_r\left(\dot{\theta}\dot{\psi}+\ddot{\phi}\right)-z_{fr}\left(\dot{\phi}^2+\dot{\theta}^2\right)\right]\vec{b}_3\end{aligned} \tag{4}$$

$$\begin{aligned}\vec{a}_C = & \ddot{\vec{r}}_{G/O} \\ & + \left[x_{rr}\left(\dot{\theta}^2+\dot{\psi}^2\right)-y_r\left(\dot{\theta}\dot{\phi}-\ddot{\psi}\right)+z_{rr}\left(\dot{\phi}\dot{\psi}-\ddot{\theta}\right)\right]\vec{b}_1 \\ & + \left[-x_{rr}\left(\dot{\theta}\dot{\phi}+\ddot{\psi}\right)+y_r\left(\dot{\phi}^2-\dot{\psi}^2\right)+z_{rr}\left(\dot{\phi}\dot{\psi}-\ddot{\theta}\right)\right]\vec{b}_2 \\ & + \left[x_{rr}\left(\ddot{\theta}-\dot{\phi}\dot{\psi}\right)-y_r\left(\dot{\theta}\dot{\psi}+\ddot{\phi}\right)-z_{rr}\left(\dot{\phi}^2+\dot{\theta}^2\right)\right]\vec{b}_3\end{aligned} \tag{5}$$

Using kinematics, the linear motion at the center of the body is derived as follows (Greenwood, 1988).

$$\begin{aligned}\vec{a}_G = \ddot{\vec{r}}_{G/O} = & \left(\dot{v}_x-\dot{\psi}\cdot v_y+\dot{\theta}\cdot v_z-g\cdot\sin\theta\right)\vec{b}_1 \\ & + \left(\dot{v}_y+\dot{\psi}\cdot v_x-\dot{\phi}\cdot v_z+g\cdot\sin\phi\cos\theta\right)\vec{b}_2 \\ & + \left(\dot{v}_z-\dot{\theta}\cdot v_x-\dot{\phi}\cdot v_y+g\cdot\cos\phi\cos\theta\right)\vec{b}_3\end{aligned} \tag{6}$$

2.2. Problem Assumptions

If $\vec{a}_G$ in Equation (6) can be measured by using a 2-axis accelerometer, both pitch and roll can be calculated respectively as follows

$$\theta = \sin^{-1}\left(\frac{\dot{v}_x-\vec{a}_G\cdot\vec{b}_1-\dot{\psi}\cdot v_y-\dot{\theta}\cdot v_z}{g}\right) \tag{7}$$

$$\phi = \sin^{-1}\left(\frac{\vec{a}_G\cdot\vec{b}_2-\dot{v}_y-\dot{\psi}\cdot v_x+\dot{\phi}\cdot v_z}{g\cos\theta}\right) \tag{8}$$

We may encounter two main problems when calculating pitch and roll with Equations (7) and (8). The first is whether the available sensors are capable of measuring all possible information, the second is how well the sensors can perform in the presence of measurement noise and disturbances coming from a running engine and a road surface. To reduce the number of sensors without exacerbating the first problem, it is assumed that the vehicle is driven on a highway with relatively slow changes in yaw. Thus, v_y, $\dot{v}_y$ and v_z are small and can be neglected. According to this driving scenario, Equation (7) and (8) can be approximated respectively as follows

$$\theta \cong \sin^{-1}\left(\frac{\dot{v}_x-\vec{a}_G\cdot\vec{b}_1}{g}\right)+v_\theta \equiv \theta_{meas}+v_\theta \tag{9}$$

$$\phi \cong \sin^{-1}\left(\frac{\vec{a}_G\cdot\vec{b}_2-\dot{\psi}\cdot v_x}{g\cos\theta}\right)+v_\phi \equiv \phi_{meas}+v_\phi \tag{10}$$

where θ_{meas} and ϕ_{meas} represent the approximated pitch and roll respectively based on sensor measurements.

To calculate both θ_{meas} and ϕ_{meas} above, it is assumed that GPS is implemented to obtain absolute velocity (v_x) and its derivative ($\dot{v}_x$), and both a 2-axis MEMS accelerometer and a yaw rate sensor are placed at point G. In addition, it is assumed that the vehicle contains 2-axis MEMS accelerometers at points A, B, C and a roll rate sensor at point G. The second problem above, which concerns measurement noise, is addressed by the use of an estimation algorithm that uses these additional sensors to reduce the effect of sensor noise and disturbances. The operation of this algorithm is described in the next section.

3. ESTIMATION ALGORITHM

The proposed estimation algorithm to minimize the effect of noise and disturbances is composed of two sequential signal processing filters. The first filter is a pre-signal processing filter to reduce the effects of measurement noise and wireless communication noise. The second filter is a discrete Kalman filter to minimize the effect of road disturbances and engine noise.

3.1. Pre-signal Processing

When the acceleration at points A, B and C is measured and all measurements are transferred via wireless S/N, there exist two main types of noise to be considered: one is due to wireless networks and the other results from both measurement noise and disturbances in a vehicle. When wireless networks are used, packet loss is one of most important issues to be considered. In general, the packet loss is related to the sampling time. That is, the faster the data are sampled, the more frequently packet loss may occur. As listed in Table 1, when MICAz is used as an S/N system, the experimental results show less than 5% packet loss if the sampling time is larger than 30 (ms) (refer to Figure 3). Therefore, 30 (ms) was used as the sampling time for the experiments described later.

The second main type of noise comes from system disturbances as well as electrical measurement noise. For instance, an engine running in a vehicle vibrates the entire vehicle. Using Equation (9) and (10) and sensor measurements in a stationary vehicle, we can calculate both θ_{meas} and ϕ_{meas}. When the result in Figure 4(a) is compared with that in Figure 4(b), it is clear how much the noise characteristics are changed due to engine vibration. For this reason, a moving average filter for the pre-signal processing step is used due to its simplicity, as follows (Smith, 1999):

$$y(k) = \frac{1}{m+1}\sum_{i=0}^{m} x(k-i) \tag{11}$$

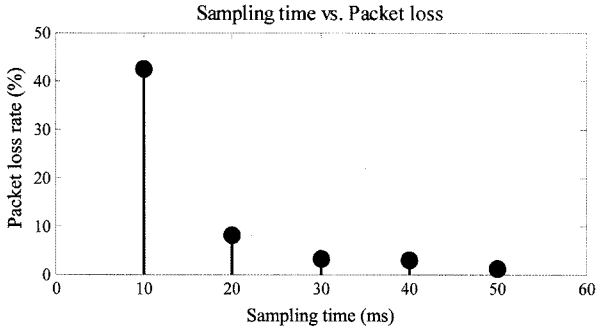

Figure 3. Sampling time vs. packet loss.

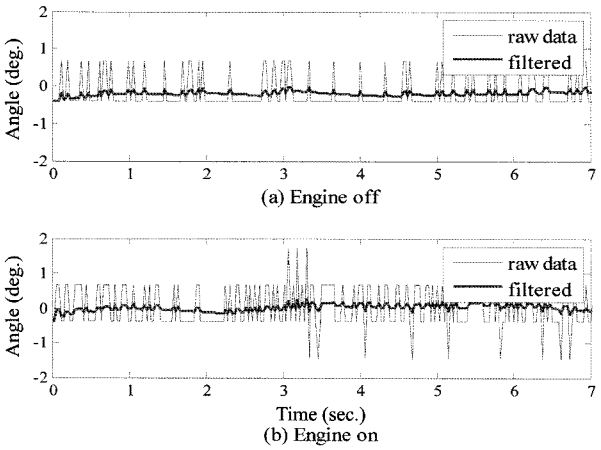

Figure 4. Noise cancellation via a pre-signal-processing filter in a stationary vehicle.

When seven data points are chosen for the moving average (i.e., m=7), the measurement noise can be cancelled out in the stationary vehicle, as shown in Figure 4(a). Furthermore, Figure 4(b) shows that the measurement noise can be also reduced via the pre-signal processing step even in the presence of engine vibration.

Consequently, we can preprocess the acceleration at each sensor node after filtering the measurement with a 30 (ms) sampling time using the moving average filter. In practice, measured accelerations at the points A, B and C are affected by road disturbances and noises coming from the running engine during acceleration. In the next section, a discrete Kalman filter is proposed to reduce this noise and road disturbance.

3.2. Estimation of Pitch Angle

A pair of accelerometers can be used to measure and/or estimate pitch rate without requiring a gyroscope. That is, the relative acceleration information includes angular velocity and acceleration of the vehicle. More specifically, when two accelerations at points B and C are subtracted (refer to Equation (4) and Equation (5)), the relative acceleration is written as

$$[\vec{a}_B - \vec{a}_C]\cdot\vec{b}_3 = (x_{fr} + x_{rr})(\dot{\phi}\dot{\psi} - \ddot{\theta}) - (z_{fr} - z_{rr})(\dot{\phi}^2 + \dot{\theta}^2) \quad (12)$$

where $[\vec{a}_B - \vec{a}_C]\cdot\vec{b}_3$ is the dot product of two vectors. Since $z_{fr} - z_{rr} \approx 0$, the angular acceleration of pitch can be calculated as

$$\ddot{\theta} = \dot{\phi}\dot{\psi} - \frac{[\vec{a}_B - \vec{a}_C]\cdot\vec{b}_3}{x_{fr} + x_{rr}} \quad (13)$$

However, since the measured value of $\ddot{\theta}$ contains both bias and noise in general, it can be written as (Ryu and Gerdes, 2004)

$$P_m = \ddot{\theta} + P_{bias} + w_\theta \quad (14)$$

Equation (14) can then be represented in state space form as follows

$$\begin{bmatrix} \dot{\theta} \\ \ddot{\theta} \\ \dot{P}_{bias} \end{bmatrix} = \begin{bmatrix} 0 & 1 & 0 \\ 0 & 0 & -1 \\ 0 & 0 & 0 \end{bmatrix} \begin{bmatrix} \theta \\ \dot{\theta} \\ P_{bias} \end{bmatrix} + \begin{bmatrix} 0 \\ 1 \\ 0 \end{bmatrix} P_m + \begin{bmatrix} 0 \\ 1 \\ 0 \end{bmatrix} w_\theta \quad (15)$$

$$\Rightarrow \dot{x} = Ax + B_u u_\theta + B_w w_\theta$$

where, $x = [\theta \ \dot{\theta} \ P_{bias}]^T \in \mathbf{R}^3$, $u_\theta = P_m \in \mathbf{R}$. Moreover, the output is the pitch angle based on Equation (9) and given as

$$y = [1 \quad 0 \quad 0]x = Cx = \theta_{meas} + v_\theta \quad (16)$$

The algorithm to estimate both pitch and pitch rate will now be derived using a Kalman filter in the discrete time domain. First of all, if Equation (15) is discretized for the given sampling time, the system is of the form (Ryu and Gerdes, 2004)

$$\hat{x}(k+1|k) = A_d\hat{x}(k|k) + B_d u(k) \quad (17)$$

where $A_d = e^{A\Delta t}$, $B_d = \int_0^{\Delta t} e^{A\tau} B d\tau$. When the discrete Kalman filter is adapted, the algorithm is

$$\begin{aligned} \hat{x}(k+1|k) &= A_d\hat{x}(k|k) + B_d u(k) \\ \hat{x}(k+1|k+1) &= \hat{x}(k+1|k) + K\{y(k+1) - C\hat{x}(k+1|k)\} \end{aligned} \quad (18)$$

where K is calculated by solving a Riccati equation. It should be noted that the proposed algorithm is designed to estimate both pitch and pitch rate by combining θ_{meas} with a kinematic relationship between acceleration measurements at sensor nodes. If a dynamic model including a suspension model is available, it can be incorporated with the above algorithm and may result in better performance. However, this dynamic model is dependent on the type of vehicle, and its specific parameters are generally confidential. Thus, the estimation algorithm, which applies kinematics to sensor node locations, is

proposed here despite some sacrifice of performance.

3.3. Estimation of Roll Angle

While the pitch angle estimation algorithm uses pitch angular acceleration (since the sensor to measure pitch rate is not available in a commercial vehicle), roll rate sensors for roll stability control have been implemented and their information is available via in-vehicle communication. This roll rate information can thus be used directly to estimate roll angle. The measurement for the roll rate sensor can be described as

$$Q_m = \dot{\phi} + Q_{bias} + w_\phi \tag{19}$$

Equation (19) can then be written in state space form as follows

$$\begin{bmatrix} \dot{\phi} \\ \dot{Q}_{bias} \end{bmatrix} = \begin{bmatrix} 0 & 1 \\ 0 & 0 \end{bmatrix} \begin{bmatrix} \phi \\ Q_{bias} \end{bmatrix} + \begin{bmatrix} 1 \\ 0 \end{bmatrix} Q_m + \begin{bmatrix} 1 \\ 0 \end{bmatrix} w_\phi \tag{20}$$

and Equation (20) can be rewritten as

$$\begin{aligned} \dot{p} &= Ap + B_u u_\phi + B_w w_\phi \\ q &= [1 \;\; 0]p = \phi_{meas} + v_\phi \end{aligned} \tag{21}$$

where $p = [\phi \;\; Q_{bias}]^T \in \mathbf{R}^2$, $u_\phi = Q_m \in \mathbf{R}$, and q is the output. While θ_{meas} is obtained by Equation (10), the pitch angle is not measurable. However, if the estimate of the pitch angle from Equation (18) is used, the output measurement can be described as

$$\phi_{meas} \cong \sin^{-1}\left(\frac{a_{y,meas} - \dot{\psi} v_x}{g \cos\hat{\theta}} \right)$$

where $\hat{\theta}$ is the estimate of θ using Equation (18). As is done for the pitch estimation, roll can be estimated sequentially using the discrete Kalman filter similarly derived in Equation (18).

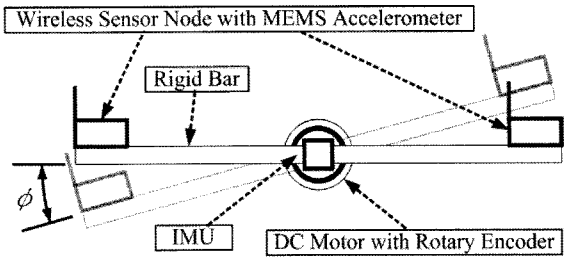

Figure 5. Schematics of indoor test platform.

4. EXPERIMENTAL VALIDATION

To validate the proposed estimation algorithm, two test platforms were used: the first is an indoor test platform in which the estimated and measured values can be compared under ideal environments. The second is a vehicle test platform, that allows us to evaluate the estimation algorithm in a real vehicle.

4.1. Validation via an Indoor Test

As shown in Figure 5, the indoor test platform consists of a rigid bar with length of 1.2 m, an S/N system, a motor, and sensors. A pair of sensor network nodes including a 2-axis MEMS accelerometer and a wireless communication module are placed on the end of the bar, and the rotary encoder is placed on the center of the bar to measure rotating angle. The indoor test platform is intended to validate how well the proposed algorithm, which is based on a pair of sensor network nodes, estimates the rotating angle. Furthermore, an IMU is

Table 1. Hardware specifications for experiments.

Type	Model	Specification	Manufacturer
Encoder	MR type L	Pulse per Revolution: 5376 (Pulse × Gear ratio)	maxon motor
S/N	MICAz	Processor: ATMega128L IEEE 802.15.4, 2.4 GHz RF Communication	Crossbow
Accelero-meter	ADXL202	Range: ±2g Sensitivity: 12.5%/g Sensitivity Accuracy: ±16%	Analog Device
IMU	MTi	Resolution: 0.05° RMS Static Accuracy: <0.5° Dynamic Accuracy: 2° RMS	Xsense
GPS	VBOX	Update rate: 100 Hz Velocity Accuracy: 0.028 m/s 16 bit analog output	Racelogic

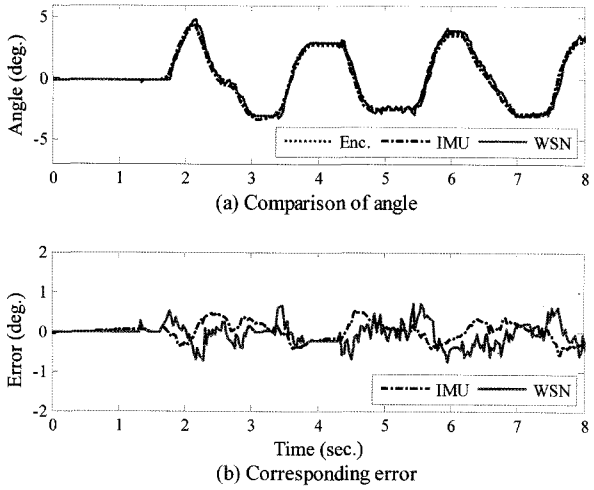

Figure 6. Estimated angle and the corresponding error for 0.5 Hz excitation.

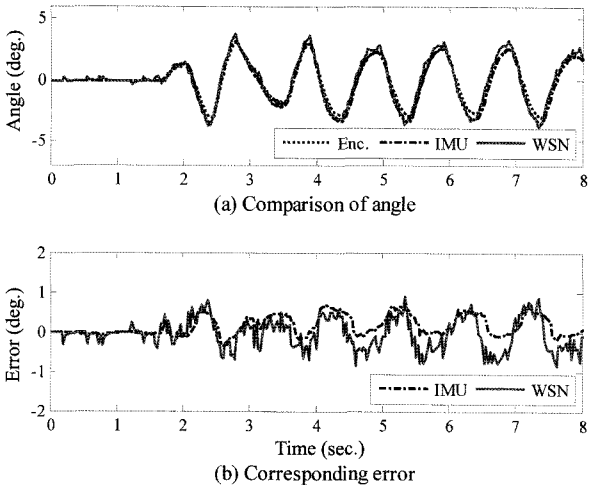

Figure 7. Estimated angle and corresponding error for 1 Hz excitation.

equipped to validate algorithm performance and is later used as a 2-axis accelerometer to measure linear acceleration at the center of the rigid body in the road test using a real vehicle. Table 1 shows a list of the hardware used for the indoor and road tests.

Since it is reported that the natural frequency of passenger vehicles is designed to be approximately 1(Hz) to avoid road vibration resonance (Gillespie, 1992), two different frequencies of excitations are used to validate the proposed algorithm. Shown in Figure 6 are the time responses of the estimated angle and angular rate when the rod in the indoor test platform was excited with a frequency of 0.5 (Hz) and a ±4 (degree) amplitude with a DC motor. It is clear that the performance both of the pitch estimation algorithm based on wireless S/N and of the IMU are quite similar and that their estimation errors with respect to the encoder measurement are within 0.7 (degree). When an excitation frequency of 1 (Hz) and a ±4 (degree) amplitude were applied, the estimation errors of the pitch estimation algorithm via S/N and the IMU with respect to the encoder measurement were less than 0.8 (degree), as shown in Figure 7.

Since the performance of the estimation algorithm relies on design parameters such as the number of data points in Equation (11) and the Kalman filter gain (K) in Equation (18), these parameters should be tuned for the given environment. For example, the Kalman filter gain K is obtained by solving a Riccati equation for the given $\sigma(v)=0.0005$. The noise characteristics can be determined by analyzing the signal from a sensor network node, which includes measurement and communication noise. Since additional disturbances due to a running engine and/or irregular road surface are added to a vehicle traveling on a real road, an analysis of noise characteristics was performed for the road test and is described later. Finally, the number of data points is related to robustness and the rate of convergence. That is, as m decreases, the rate of convergence improves while the noise cancellation performance is degraded.

4.2. Feasibility via Road Tests

While the estimation algorithm was validated above in the ideal environment, it is necessary to test its performance in the real driving environment. Figure 8 shows the test vehicle platform manufactured by Hyundai Motors that includes S/N nodes and an IMU. The corresponding dimensions of the sensor array are as follows

$x_{fr}+x_{rr}=3.36m$, $y_l+y_r=1.47m$, and $z_{fr}-z_{rr}=0$

Furthermore, the design parameters for the experimental tests are chosen as follows:

$m = 7$
$K_\theta = [0.03\ 0.15\ 0.00006]^T$
$K_\phi = [0.035\ 0.00035]^T$

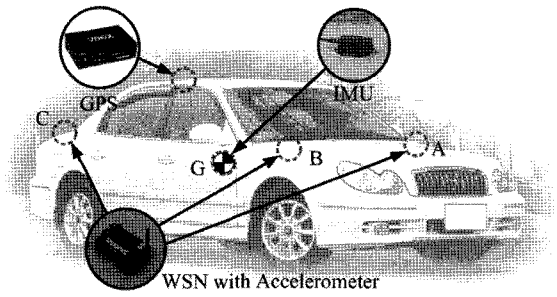

Figure 8. Test vehicle platform.

To validate the proposed estimation algorithm, three driving scenarios were developed to compare the perfor-

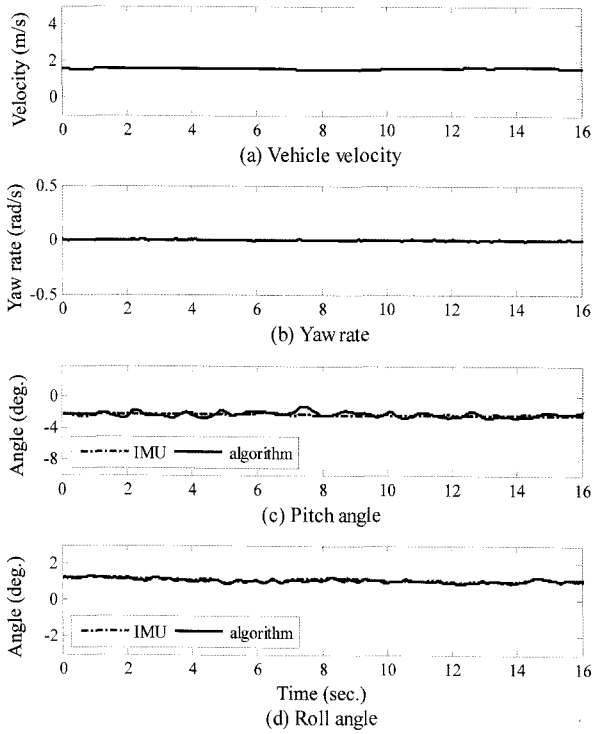

Figure 9. Estimation of roll and pitch without longitudinal acceleration and yaw motion.

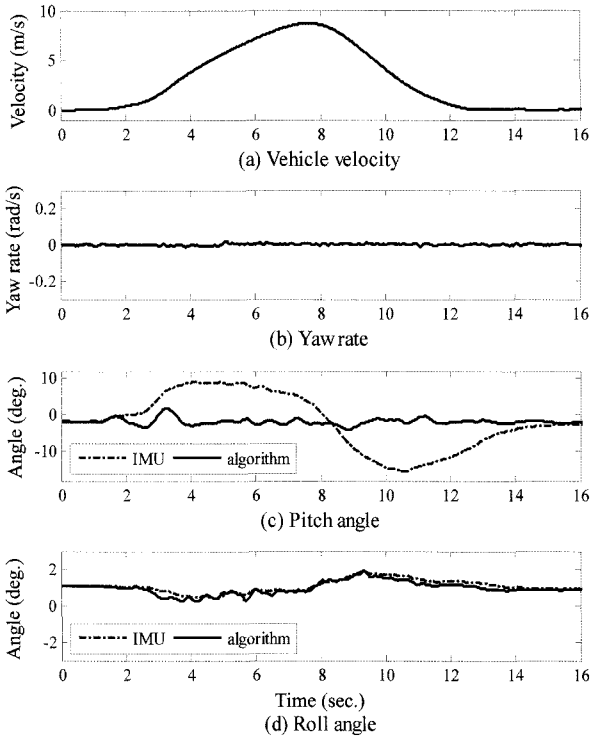

Figure 10. Estimation of roll and pitch with longitudinal acceleration and without yaw motion.

mances of the proposed algorithm and the IMU in estimating roll and pitch. The first case is that of a vehicle operated with almost constant speed and without yaw motion. This test attempts to show that both algorithms work well under ideal driving conditions and can provide estimates of pitch and roll angles for the given road condition. The second and third scenarios incorporate longitudinal acceleration and/or yaw motion respectively. These field tests are designed to show the extent to which the performance of the IMU may be degraded under the given driving scenario and to what degree the proposed algorithm can compensate for degradation based on the results from the first driving test. It is noted that each driving scenario was tested at least five times under the same road conditions.

For the first driving scenario under the default road conditions, the estimates of roll and pitch angles are about 1.0 and –2.0 (degree) respectively as shown in Figure 9. Both the proposed algorithm and the IMU show similar performance. More precisely speaking, the IMU gives a slightly better performance for the pitch estimation because the pitch rate is available only to the IMU. Although commercial vehicles are generally not equipped with pitch rate sensors, it is expected that the proposed algorithm can be improved once these sensors are implemented in vehicles.

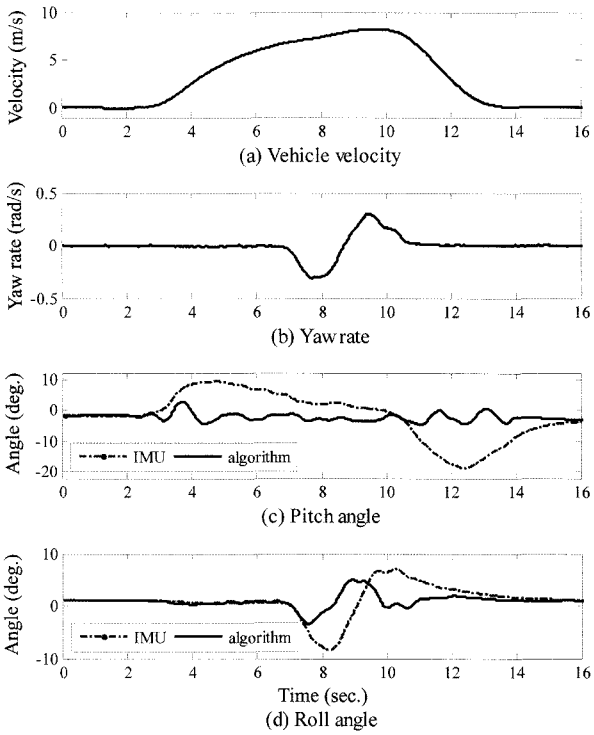

Figure 11. Estimation of roll and pitch with longitudinal acceleration and yaw motion.

In the second scenario, the vehicle moved without yaw motion but started to accelerate after 3 seconds as shown in Figure 10(a). Both the proposed algorithm and the IMU show similar performance in estimating roll angle in this scenario because the yaw rate is approximately zero during the test (refer to Figure 10(d)). However, the IMU estimates the pitch angle with more than ±10 (degree) of variation due to the longitudinal acceleration. Based on the experimental results in Figure 9(c), the pitch angle estimated by the IMU is physically unrealistic for the terrain. In contrast, the proposed algorithm estimates the pitch angle with less than ±2.0 (degree) of variation, which is similar to the result in Figure 9(c).

In the third scenario, the vehicle moved with yaw motion and accelerated after 3 seconds, as shown in Figures 11(a) and 11(b). As expected, the performance of the IMU in estimating both pitch and roll is degraded in both directions. That is, the estimated roll angle varies by about ±10 (degree) due to steering, and the estimated pitch angle changes between 10 and −20 (degree). Both results show a high amount of estimation error. In contrast, the estimated values generated by the proposed algorithm show a much smaller amount of error. We conclude therefore that the performance of the proposed algorithm is better than that of the IMU in more diverse driving environments such as those including longitudinal acceleration and/or yaw motion.

5. CONCLUSION

This paper presented a new algorithm to estimate both roll and pitch of a passenger vehicle using an accelerometer array and sensor networks. The proposed algorithm can be divided into two procedures: the first is a pre-signal processing step in which a moving average filter is used to reduce measurement noise recorded by the sensors and S/N, and the second is an estimation step in which a discrete Kalman filter is used to combine an angle measurement with angular acceleration or angular velocity and to improve estimates of roll and pitch angle against disturbances coming from the engine and road surface. Finally, experimental tests were conducted for validation in the framework of an indoor test platform and a real vehicle. It was shown that the performance of the proposed algorithm is better than that of an IMU in realistic driving environments.

ACKNOWLEDGEMENT–This work was supported by grant No. R01-2006-000-11373-0 from the Basic Research Program of the Korea Science & Engineering Foundation.

REFERENCES

Bosch (2007). *Automotive Technology/Safety.* Bosch Website. http://rb-kwin.bosch.com/en-KR/start/safety.html

Gillespie, T. D. (1992). *Fundamentals of Vehicle Dynamics.* SAE.

Greenwood, D. T. (1988). *Principles of Dynamics*, 2nd edn. Prentice Hall. New Jersey.

Kim, M. H., Oh, J. H., Lee, J. H. and Jeon, M. C. (2006). Development of rollover criteria based on simple physical model of rollover event. *Int. J. Automotive Technology* **7**, **1**, 51–59.

Mostov, K. S., Soloviev, A. A. and Koo, T. J. (1997). Accelerometer based gyro-free multi-sensor generic inertial device for automotive applications. *Proc. IEEE Conf. ITS*, 1047–1052.

Ryu, J. and Gerdes, J. C. (2004). Integrating inertial sensors with GPS for vehicle dynamics control. *ASME J. Dynamic Systems, Measurement, and Control*, **126**, 243–254.

Siemens (2007). *Restraint Systems.* Siemens Website. http://www.siemensat.co.kr/products/ rest.html

Smith, S. W. (1999). *The Scientist and Engineer's Guide to Digital Signal Processing.* California Technical Publishing. California.

Tseng, H. E., Xu, L. and Hrovat, D. (2007). Estimation of land vehicle roll and pitch angles. *Vehicle System Dynamics* **45**, **5**, 455–443.

Ungoren, A. Y. and Peng, H. (2004). Evaluation of vehicle dynamic control for rollover prevention, *Int. J. Automotive Technology* **5**, **2**, 115–122.

VTI (2007). Product & Applications/Automotive. VTI Website. http://www.vti.fi/en/products-solutions/solutions/automotive